Plasmon Excitation Spectra for an Electron Gas with an Energy Gap

F. Bonsignori*
Institut de Physique, Strasbourg, France
and
A. Desalvo
Istituto Chimico, Facoltà di Ingegneria, Università di Bologna, Bologna, Italy and Laboratorio di Chimica e Tecnologia dei Materiali e Componenti per l'Elettronica del Consiglio Nazionale delle Ricerche, Bologna, Italy
(Received 16 April 1970)

The plasmon excitation spectrum of an electron gas in a real crystal is analyzed in the random-phase approximation without exchange for the weak-binding case. The features of this spectrum are studied as a function of energy gap and electron density. Several plasmon branches, which do not always go down to $q=0$, appear with increasing energy gap and with the filling of the valence band. The contribution of normal and umklapp processes to the behavior of the real part of the dielectric constant is analyzed and correlated with a phenomenological model.

I. INTRODUCTION

In a recent paper, we evaluated the energy loss of protons to valence electrons in solids under channeling conditions.[1] The model took into account an electron gas having a space-periodic density and allowed evaluation of the off-diagonal matrix elements of the response function.

The analysis of the excitation spectrum in our particular case showed a very different behavior both from the familiar free-electron case[2] and from another one studied by other authors.[3] The latter found for the first time a collective state at intermediate q values as a consequence of the interaction of the periodic potential with the electron gas. In our case, however, the two branches of the plasmon excitation line did not join through the continuous single-particle excitation spectrum, and the upper branch did not go down to momentum transfers $\vec{q}=0$, but gave rise to a closed loop.

Therefore we thought it beneficial to study the interrelation among the various particular cases reported up to now by different authors.[1-4] For this purpose a systematic analysis of the excitation spectrum has been carried out by varying some of the parameters which characterize the electron gas in real crystals (energy gap, electron density). In particular, cases very similar to the ones previously treated, i.e., metals with a small energy gap[3] and semiconductors,[4] have been included.

We recall here briefly the essential features and approximations of the model employed in Ref. 1. The response function was calculated in the random-phase approximation (RPA) without exchange for the nearly-free-electron case.[1,5,6] The model was particularized for s electrons in gold and the parameters chosen accordingly. The simple spherical Penn model[7] was modified in order to take into account crystal anisotropy. The Brillouin zone was still assumed as a sphere of equal volume partitioned, however, in 14 equivalent sectors, one for each first and second neighbor of the reciprocal lattice. We notice, however, that this particular assumption is of no importance in the present case, since we limit ourselves to the diagonal terms of the response function. This favorable circumstance arises from the fact that for nearly free electrons with small damping, the condition for plasmon existence is still determined by the usual condition[1]

$$\epsilon_{0,1}=0, \tag{1}$$

where $\epsilon_{0,1}$ is the real part of the diagonal dielectric constant. In fact, in the weak-binding approximation, the response function is of the form[1,5]

$$\mathcal{K}(\vec{q},\vec{G},\omega)=\delta_{\vec{G},0}\frac{1}{1+\alpha(\vec{q},0,\omega)}-(1-\delta_{\vec{G},0})\times\frac{\alpha(\vec{q},\vec{G},\omega)}{1+\alpha(\vec{q},0,\omega)}\,, \tag{2}$$

where $\alpha(\vec{q},\vec{G},\omega)$ are the polarizability components corresponding to the reciprocal lattice vector $\vec{G}$:

$$\alpha(\vec{q},\vec{G},\omega)=-\frac{4\pi e^2}{\Omega|\vec{q}+\vec{G}|^2}\sum_{j,\beta}\langle\beta|\exp(i\vec{q}\cdot\vec{r})|j\rangle\times\langle j|\exp[-i(\vec{q}+\vec{G})\cdot\vec{r}]|\beta\rangle\times\left(\frac{1}{\hbar\omega-(E_\beta-E_j)+i\eta}-\frac{1}{\hbar\omega+(E_\beta-E_j)+i\eta}\right) \tag{3}$$

(where Ω is the volume and j, β are initial and final states, respectively). In particular, for free electrons

$$\epsilon(\vec{q},\omega)=1+\alpha(\vec{q},0,\omega)\,. \tag{4}$$

Therefore the singularities of the response function are the same as for the usual case $\vec{G}=0$.

Obviously in a real crystal, plasmons can be damped due to U processes. However, under the

assumption of small damping, the dispersion relation of the real part of plasma frequency is still given by (1) (see Ref. 2, p. 176).

Therefore, in order to determine the plasmon excitation spectrum, it is sufficient to calculate $\epsilon_{0,1}$ as a function of $\vec{q}$ and ω.

II. DESCRIPTION OF MODEL AND NUMERICAL RESULTS

In our model we introduced an energy gap for a wave vector k equal to the Brillouin-zone radius k_D. The wave function in each of the 14 sectors was assumed of the form

$$\psi_{\vec{k}} = \frac{1}{\Omega^{1/2}} \frac{e^{i\vec{k}\cdot\vec{r}} + C_{\vec{k}} e^{i(\vec{k}+\vec{G})\cdot\vec{r}}}{(1+C_{\vec{k}}^2)^{1/2}}, \tag{5}$$

where the symbols have the same meaning as in Ref. 1. In particular, $\vec{G} = -2k_D\hat{k}$, where $\hat{k}$ is a unit vector in the direction of the reciprocal-lattice vector lying in the same sector of $\vec{k}$. This point differs from the isotropic Penn's model, in which $\hat{k}$ is simply directed along $\vec{k}$.[7]

Moreover, for $k > 2k_D$ we assumed free-electron behavior. We took into account both normal and umklapp processes. We assumed an extended zone scheme and, as usual (see, e.g., Ref. 7) we refer to transitions for which $\vec{G} = 0$ as "normal" and these for which $\vec{G} \neq 0$ as "umklapp." Consistently with our model, the latter can occur only up to momentum transfers $q > 2k_D$.

As in our previous paper, we use here nondimensional units $2k_D = 3.04$ Å^{-1} for wave vectors and

$$4E_D = 4\hbar^2 k_D^2/2m = 34.8 \text{ eV}$$

for energies. With these units, the parameter $\chi^2 = (\pi a_0 k_F)^{-1}$ (where a_0 = Bohr radius) used by other authors[4,8] turns out to be $\chi^2 = 0.198/k_F$, where k_F is in our nondimensional units.

The two variables considered here were the energy gap E_g and the Fermi radius k_F: We varied either of them, keeping the other one fixed. Starting from the values of the parameters previously used [Ref. 1; energy gap $E_g = 0.17$, Fermi wave vector $k_F = 0.4$ (half-full band)] we extended the analysis to E_g values ranging from the free-electron case ($E_g = 0.0$) up to fairly-high-energy gaps ($E_g = 0.25$, i.e., $E_g = E_D$), keeping the electron density constant. A further extension to higher-energy gaps does not seem consistent with weak-binding assumption. Moreover, the case in which the filling of the band varies from the semiconductor case (full band) down to a fairly empty band ($k_F = 0.3$, i.e., about $\frac{1}{5}$ full) keeping E_g constant was considered.

The real part of the dielectric constant was evaluated by numerical integration using a digital computer. Calculations were performed partly on the CDC 6600 of the University of Bologna and partly

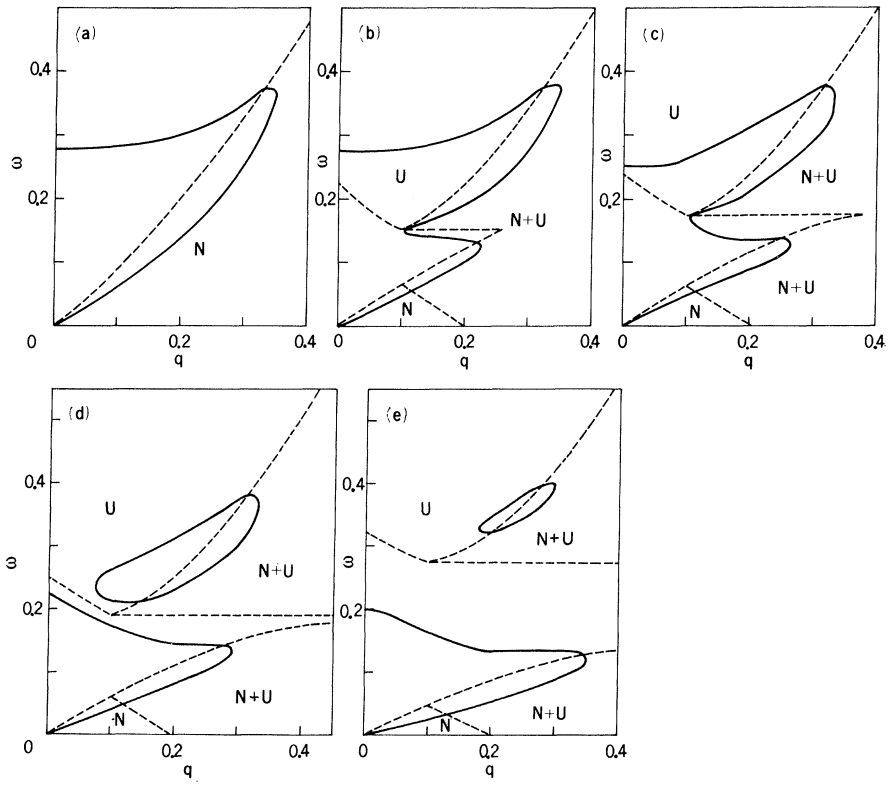

FIG. 1. Plasma excitation spectrum as a function of energy gap with constant electron density ($k_F = 0.4$). Along the full line $\epsilon_{0,1} = 0$; dashed lines bound the single-particle excitation spectrum and N and U indicate normal and umklapp processes, respectively. (a) $E_g = 0.0$; (b) $E_g = 0.10$; (c) $E_g = 0.13$; (d) $E_g = 0.15$; (e) $E_g = 0.25$. (ω and q as well as E_g and k_F in nondimensional units, see text.)

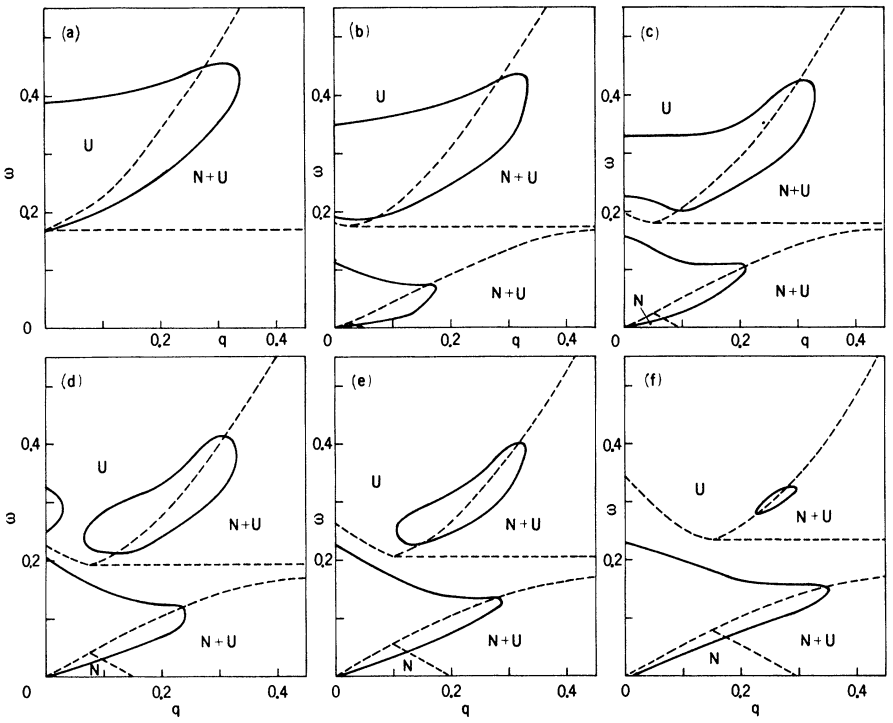

FIG. 2. Same as Fig. 1, but as a function of electron density with constant energy gap ($E_g = 0.17$); (a) $k_F = 0.5$; (b) $k_F = 0.475$; (c) $k_F = 0.45$; (d) $k_F = 0.425$; (e) $k_F = 0.4$; (f) $k_F = 0.35$. (ω and q as well as E_g and k_F in nondimensional units, see text.)

on the IBM 360/65 of the Nuclear Centre of Kronenboug (Strasbourg).

Figure 1 shows the behavior of the excitation spectrum with increasing energy gap, keeping the lower band half-full.

In Fig. 1(a) one sees the spectrum for $E_g = 0$, with the usual plasmon branch. With the introduction of an energy gap, the single-particle excitation spectrum shows a gap limited to a narrow q range: Inside this region a new plasmon branch appears [Fig. 1(b)]. This branch corresponds to the "zone-boundary collective state" found by other authors.[3] We notice that for these not-too-high values of E_g the two branches join continuously through the single-particle excitation spectrum.

With increasing E_g, ω_p at $q = 0$ decreases [Fig.

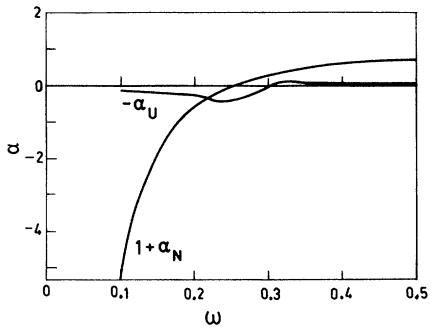

FIG. 3. Contributions to the real part of dielectric constant vs ω. α_N and α_U are the contributions due to N and U processes, respectively. $E_g = 0.17$, $k_F = 0.4$, $q = 0.025$. (ω and q as well as E_g and k_F in nondimensional units, see text.)

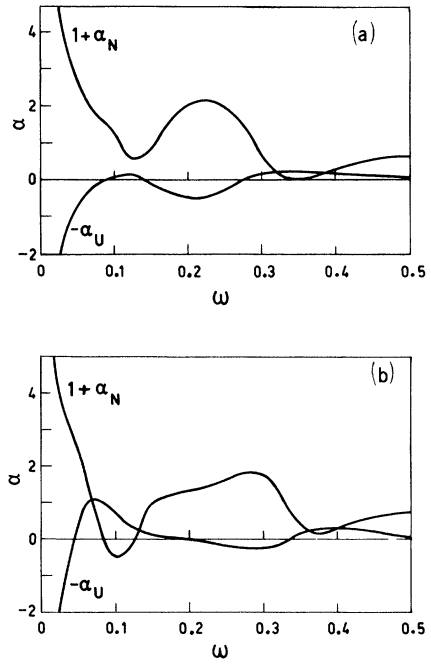

FIG. 4. Same as Fig. 3 for (a) $E_g = 0.17$; $k_F = 0.4$; $q = 0.3$: (b) $E_g = 0.25$, $k_F = 0.4$, $q = 0.275$.

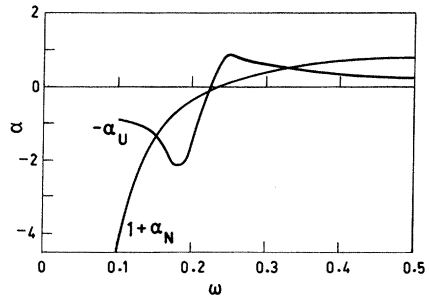

FIG. 5. Same as Fig. 3 for $E_g = 0.17$; $k_F = 0.45$; $q = 0.025$.

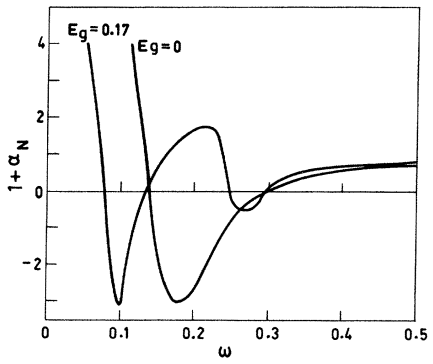

FIG. 7. Same as Fig. 6, but for $q = 0.2$.

1(c)] and finally, concurrently with the appearance of an energy gap in the single-particle excitation spectrum, the two branches split [Fig. 1(d)]. The zone-boundary collective state ranges up to $q = 0$, while the upper branch becomes a closed loop without reaching low-q values any more. This corresponds to the case previously treated by us.[1] A further increase of E_g makes the loop shrink and the upper plasmon branch tends to disappear [Fig. 1(e)].

Figure 2 shows the variation of the spectrum when the band is progressively emptied for the particular E_g used in our previous paper. Figure 2(a) corresponds to a lower band completely filled, i.e., to the more usual case of a semiconductor.[4] Also in this case we have a single plasmon branch. The essential difference compared to free electrons lies in the fact that the line $\epsilon_{0,1} = 0$ does not go through the origin. This is strictly correlated with the well-known fact that the limit of $\epsilon_{0,1}(0, \omega)$ when $\omega \to 0$ is finite (incomplete static screening).[7,9] Obviously, in this case only excitations corresponding to interband transitions are present. As the band becomes more and more empty, an intraband excitation spectrum and correspondingly a plasmon branch, separated from the other, appear [Fig. 2(b)]; this branch expands with decreasing k_F [Fig. 2(c)]. The transition between this type of excitation spectrum and that with a closed loop, in which the upper plasmon branch does not reach the point $q = 0$ any more, is shown clearly in Fig. 2(d). The upper branch splits off and gives rise to a closed loop. In a narrow region of small q values, a plasmon branch still survives, which, however, disappears as k_F decreases: Then we obtain again the case previously treated by us[1] [Fig. 2(e)]. As k_F decreases further, the closed loop shrinks more and more and finally disappears [Fig. 2(f)].

III. DISCUSSION

Our results can be correlated on the basis of the simple phenomenological model proposed by Wilson.[10] In this model, the real behavior of the electron gas is approximated by two sets of oscillators, one representing free electrons, the other representing bound electrons which can undergo transitions which give rise to an optical absorption band. The behavior of the zeros of the real part of the dielectric constant is analyzed as a function of the relative position of the free-electron plasma frequency and the optical absorption band, and of the width and intensity (i.e., the oscillator strength) of the latter.

It is convenient to separate the contribution of

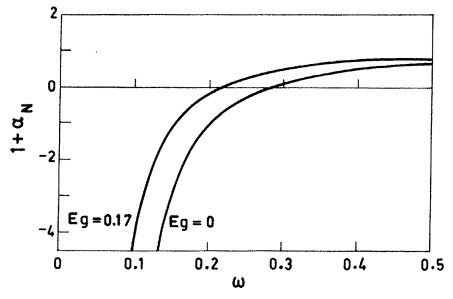

FIG. 6. $1+\alpha_N$ for $k_F = 0.4$; $q = 0.1$ and two different values of $E_g = 0.0$ and $E_g = 0.17$ (ω and q as well as E_g and k_F in nondimensional units, see text.)

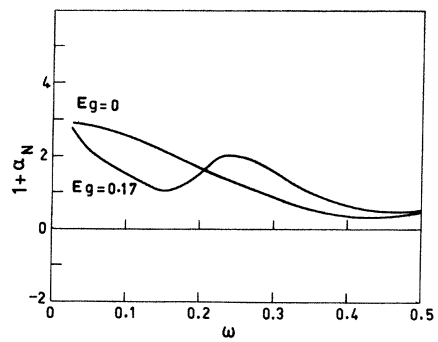

FIG. 8. Same as Fig. 6, but for $q = 0.4$.

normal and umklapp processes to dielectric constant in the following form:

$$\epsilon_{0,1} = 1 + \alpha_N + \alpha_U , \tag{6}$$

where N stands for normal and U for umklapp. Generally, the contribution of α_U is on the average about 20% and can be considered a small correction. However, in some cases which are of particular interest here ($\epsilon_{0,1} \sim 0$) this is no longer true. This occurs when E_g is sufficiently great ($E_g \geq 0.15$) and the band is full enough ($k_F \simeq 0.4$). In these regions α_U produces the following effects:

(i) For small q (here and in the following, for "small" q we mean $q \leq k_D - k_F$, i.e., q is inadequate for producing normal interband transitions) a noticeable shift in the zero of $\epsilon_{0,1}$ occurs ($\Delta\omega_p \simeq 0.04$, see Fig. 3).

(ii) For large q ($q \simeq 0.3$), α_U, even though small, maintains two zeros at large ω in $\epsilon_{0,1}$ which otherwise will tend to disappear in $1 + \alpha_N$ [Fig. 4(a)]. This causes the loop to be larger and, indeed, to persist up to high values of E_g [$E_g \simeq 0.25$, Fig. 4(b)].

A third and more considerable effect occurs when the band becomes even fuller ($k_F \simeq 0.45$). In this case for small q, $\alpha_U(\omega)$ is of the same order of $1 + \alpha_N(\omega)$ over an extended ω region and varies strongly with frequency. It behaves as in the case treated by Wilson when a broad and strong optical absorption band is present, [see Figs. 3, 4(a), and 5(a) of Ref. 10] which splits the plasma frequency in three (Fig. 5), giving rise to the plasmon branches of Figs. 2(b) and 2(c).

Now we analyze the behavior of $1 + \alpha_N(\omega)$. For small q values it does not depart greatly from the free-electron case. However, the curves show a general shift towards lower ω values which increases with q (see Fig. 6); this occurs concurrently with the depression to lower ω values of the intraband excitation spectrum compared to the free-electron case (see Fig. 1).

For q high enough to produce normal interband transitions, the behavior is very complicated. By comparing with the free-electron case, one can regard the trend as being due to a superposition of a free-electron-like curve and an optical absorption band (Fig. 7). As a consequence, in agreement with the Wilson model's expectations for the case of a strong optical absorption band, the plasma frequency splits again in three frequencies (possibly shifted by U processes). With increasing q this oscillation in $1 + \alpha_N$ damps out, i.e., the oscillator strength for interband transitions decreases, and $1 + \alpha_N$ tends again to become free-electron-like (Fig. 8).

In conclusion, our results show that as the energy gap and the electron density vary, the plasmon excitation spectrum varies much more markedly than one could expect on the basis of the simple cases usually considered, i.e., the free-electron gas and the semiconductor.

The main features which can be present are:

(i) a plasmon branch at intermediate q values (zone-boundary collective state), which joins to the ordinary branch through the single-particle excitation spectrum,

(ii) a closed loop which does not reach $q = 0$,

(iii) three plasma frequencies at $q = 0$.

In the first two cases, the presence of several plasmon branches for intermediate and large q is essentially due to the occurrence of normal interband transitions. Umklapp processes play a minor role, which, however, becomes more important with increasing E_g. In this case the shift of ω_p at small q's turns great enough to produce the excitation spectrum with a closed loop.

In fact, in our nearly-free-electron model this contribution depends on the $C_{\vec{k}}^2$'s [see Eq. (8) of Ref. 1]: When k_F increases, electronic states which lie nearer to the zone boundary and therefore have a greater $C_{\vec{k}}$ contribute to these processes.

It is important to point out once more the limitations of our model: Actually the crystal symmetry has been considerably underestimated, and the treatment was restricted to nearly free electrons. Furthermore, the lattice spacing was not included among the variables. However, in spite of these simplifications, this work shows very complex features of the excitation spectrum and can give an indication of what one should expect for different real solids.

Finally, with regard to a possible comparison with experiments, recall that we were interested in the stopping power of protons under channeling conditions,[1,11] rather than in discrete energy-loss problems; however, we think that experiments aimed at checking the characteristic features outlined above are feasible and of interest. However, a proper evaluation of the damping due to interband transitions, whose importance was pointed out also recently[12,13] and which could weaken or even mask these effects, would be necessary.

---

*Permanent Address: Istituto di Fisica, Università di Bologna, Bologna, Italy, Istituto Nazionale di Fisica Nucleare, Sezione di Bologna, Bologna, Italy, and Gruppo Nazionale di Struttura della Materia del C. N. R., Italy.

[1]F. Bonsignori and A. Desalvo, J. Phys. Chem. Solids 31, 2191 (1970).

[2]D. Pines, *Elementary Excitations in Solids* (Benjamin, New York, 1963).

[3]E-Ni Foo and J. J. Hopfield, Phys. Rev. 173, 635 (1968).

[4]W. Brandt and J. Reinheimer, Can. J. Phys. 46, 607

(1968).
[5]D. S. Falk, Phys. Rev. 118, 105 (1960).
[6]G. M. Gandel'mann and V. M. Ermachenko, Zh. Eksperim. i Teor. Fiz. 45, 522 (1963) [Soviet Phys. JETP, 18, 358 (1964)].
[7]D. R. Penn, Phys. Rev. 128, 2093 (1962).
[8]J. Lindhard and A. Winther, Kgl. Danske Videnskab. Selskab, Mat.-Fys. Medd. No. 34, 4 (1964).
[9]J. M. Ziman, *Principles of the Theory of Solids* (Cambridge, U. P., London, 1964), p. 138.
[10]C. B. Wilson, Proc. Phys. Soc. (London) 76, 481 (1960).
[11]E. S. Machlin, S. Petralia, A. Desalvo, R. Rosa, and F. Zignani, Phil. Mag. 22, 101 (1970).
[12]D. F. DuBois and M. G. Kivelson, Phys. Rev. 186, 409 (1969).
[13]G. Paasch, Phys. Status Solidi 38, K123 (1970).

PHYSICAL REVIEW B VOLUME 3, NUMBER 4 15 FEBRUARY 1971

Calculation of the Temperature Dependence of the Energy Gaps in PbTe and SnTe†

Y. W. Tsang and Marvin L. Cohen
Department of Physics, University of California, Berkeley, California 94720
(Received 21 August 1970)

The empirical pseudopotential method is modified to calculate the temperature dependence of the first direct gap E_g of PbTe at the L point of the Brillouin zone. The same set of form factors which had given a reasonable band structure throughout the Brillouin zone and which adequately explains the optical properties of PbTe gives both the correct positive sign and magnitude for $(\partial E_g/\partial T)|_P$. The same method when applied to SnTe gives very unusual results, namely, a negative temperature coefficient for the region in the Brillouin zone near the minimum gap but a positive temperature coefficient for gaps slightly removed from the minimum gap. This appears to be consistent with the negative temperature coefficient obtained from tunneling experiments and the positive temperature coefficients obtained from optical measurements. The origin of the temperature dependence of conduction and valence levels at the gap is discussed in detail.

I. INTRODUCTION

Optical experiments[1,2] at constant pressure show that the first direct gap E_g of PbTe at the L point of the Brillouin zone increases linearly with temperature in the temperature range 80–350 °K; for higher temperatures, the $E_g(T)$ curve approaches a constant value. The value of the linear temperature coefficient $(\partial E_g/\partial T)|_P$ in the linear region lies between[1,2] 4.1×10^{-4} and 4.5×10^{-4} eV(°K)$^{-1}$. The positive sign of the temperature coefficient is interesting since most semiconductors have a negative temperature coefficient. In this paper, a theoretical calculation[3] of $(\partial E_g/\partial T)|_P$ for PbTe using the pseudopotential method is outlined. We obtain the correct positive sign and a value of 3.9×10^{-4} eV(°K)$^{-1}$ for $(\partial E_g/\partial T)|_P$ in the temperature range from 40 to 200 °K (Fig. 1); the slope of the theoretical curve $E_g(T)$ begins to decrease for temperature above 200 °K.

In SnTe, metal-insulator-semiconductor tunneling experiments[4] yield a negative temperature coefficient of -2×10^{-4} (°K)$^{-1}$ for the region near the minimum energy gap. This theoretical calculation of the temperature coefficient in SnTe gives a value of -1.3×10^{-4} eV (°K)$^{-1}$ for the gap at the L point of the Brillouin zone. The band structure of SnTe resembles that of PbTe throughout the zone except at

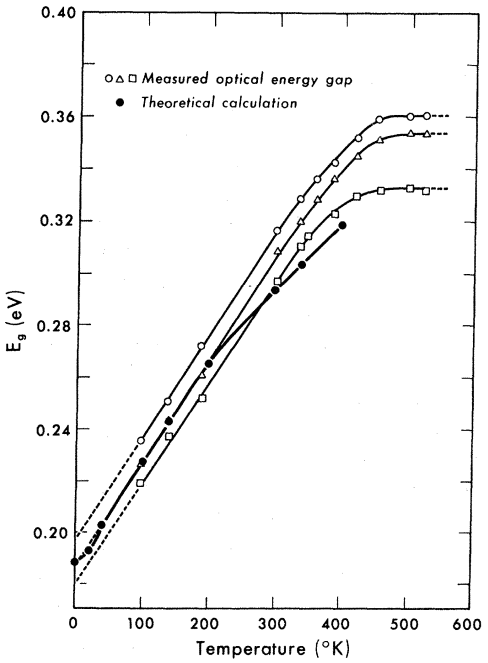

FIG. 1. Calculated and experimental temperature-dependent energy gap $E_g(T)$ for PbTe. The theoretical curve does not extend to high temperatures because Debye-Waller factors were not available above 400 °K. (The experimental data were taken from Ref. 1).